Quantitative variation in responses to root spatial constraint within Arabidopsis thaliana

Joseph, Bindu; Lau, Lillian; Kliebenstein, Daniel James

Published in:
The Plant Cell

DOI:
10.1105/tpc.15.00335

Publication date:
2015

Document version
Publisher's PDF, also known as Version of record

The Plant Cell, Vol. 27: 2227–2243, August 2015, www.plantcell.org

Quantitative Variation in Responses to Root Spatial Constraint within *Arabidopsis thaliana*[OPEN]

Bindu Joseph,[a,b] Lillian Lau,[a] and Daniel J. Kliebenstein[a,c,1]

[a] Department of Plant Sciences, University of California, Davis, California 95616
[b] Bayer Crop Science, Crop Genetics Department, Morrisville, North Carolina 27560
[c] DynaMo Center of Excellence, University of Copenhagen, DK-1871 Frederiksberg C, Denmark

ORCID IDs: 0000-0001-9298-629X (B.J.); 0000-0001-5759-3175 (D.J.K.)

Among the myriad of environmental stimuli that plants utilize to regulate growth and development to optimize fitness are signals obtained from various sources in the rhizosphere that give an indication of the nutrient status and volume of media available. These signals include chemical signals from other plants, nutrient signals, and thigmotropic interactions that reveal the presence of obstacles to growth. Little is known about the genetics underlying the response of plants to physical constraints present within the rhizosphere. In this study, we show that there is natural variation among *Arabidopsis thaliana* accessions in their growth response to physical rhizosphere constraints and competition. We mapped growth quantitative trait loci that regulate a positive response of foliar growth to short physical constraints surrounding the root. This is a highly polygenic trait and, using quantitative validation studies, we showed that natural variation in *EARLY FLOWERING3* (*ELF3*) controls the link between root constraint and altered shoot growth. This provides an entry point to study how root and shoot growth are integrated to respond to environmental stimuli.

INTRODUCTION

Plants perceive and respond to changes in their surrounding environment via an integrated suite of morphological and physiological responses to optimize their fitness (Callaway et al., 2003; Valladares et al., 2007). A key environment from which large arrays of largely uncharacterized stimuli arise is the rhizosphere. The plant has a number of systems in place to measure the quality of the rhizosphere in terms of nutrients and obstacles to growth. Changes in water or nutrient availability or presence of obstacles are perceived belowground by roots (Smith, 2000; Hodge, 2004). Additionally, competing neighbor plants can be directly perceived both above- and belowground through touch perception (de Wit et al., 2012) or volatile cues from neighboring plants (Karban et al., 2000). These chemical cues can also inform the plant about the metapopulation of microbes in the surrounding rhizosphere. Once sensed, plants respond to this multitude of rhizosphere signals by altering their shoot and root growth (Tosti and Thorup-Kristensen, 2010; Kiaer et al., 2013; Padilla et al., 2013). Interestingly, these responses vary from additive to interactive and from positive to negative effects on root or shoot growth, depending on the species or the genotype tested (Cahill et al., 2005, 2010; Murphy and Dudley, 2007; Kiaer et al., 2013). Thus, understanding the full suite of mechanisms that allow a plant to sense and respond to the rhizosphere is a significant topic in plant biology.

However, the mechanistic basis of how a plant perceives and responds to the myriad of rhizosphere-associated signals is poorly understood. Recent studies using rhizotron imaging, in which special pots are used to allow direct visualization of the roots, of roots grown in soil or artificial media showed that roots perceive the proximity to neighbors and alter their foraging behavior and architecture (Hodge, 2004; Cahill et al., 2010; Nord et al., 2011; Fang et al., 2013). While nutrient depletion is thought to be a key signal for altered root foraging in competitive environments, recent studies have shown that neighboring roots can also trigger changes in root architecture independently of nutrient competition (Padilla et al., 2013). One possible explanation arises from reports of chemical signals, such as secondary metabolites or proteins, in root exudates that mediate how a plant root interacts with its soil environment (de Kroon, 2007; Semchenko et al., 2008; Biedrzycki et al., 2010; Badri et al., 2012; Padilla et al., 2013). This agrees with evidence that roots respond to neighboring roots in a genotype-dependent manner, wherein roots of the same genotypes overlapped better, while roots of different genotypes avoided each other potentially via chemical signals (Fang et al., 2013). However, the specific molecular mechanisms involved in these processes and how they influence foliar growth are poorly understood.

Another key component of measuring the rhizosphere is the combination of gravitropism of the root and ensuing thigmotropic responses that allow the plant to detect the presence of obstructions within the soil through non-resource-based mechanisms (de Wit et al., 2012). The root's primary gravitropism and associated set point growth angle establish the initial vector for a young root's growth (Slovak et al., 2014). The root tip then perceives any ensuing obstruction to growth and alters its growth to avoid this obstruction. Therefore, the process of a plant assessing the rhizosphere involves the physical interaction with obstacles, associated avoidance, and the resulting foraging for usable space (Semchenko et al., 2008). While the root aspects of obstacle avoidance have been studied, the resulting influence on rosette growth is less well understood.

[1] Address correspondence to kliebenstein@ucdavis.edu.
The author responsible for distribution of materials integral to the findings presented in this article in accordance with the policy described in the Instructions for Authors (www.plantcell.org) is: Daniel J. Kliebenstein (kliebenstein@ucdavis.edu).
[OPEN] Articles can be viewed online without a subscription.
www.plantcell.org/cgi/doi/10.1105/tpc.15.00335

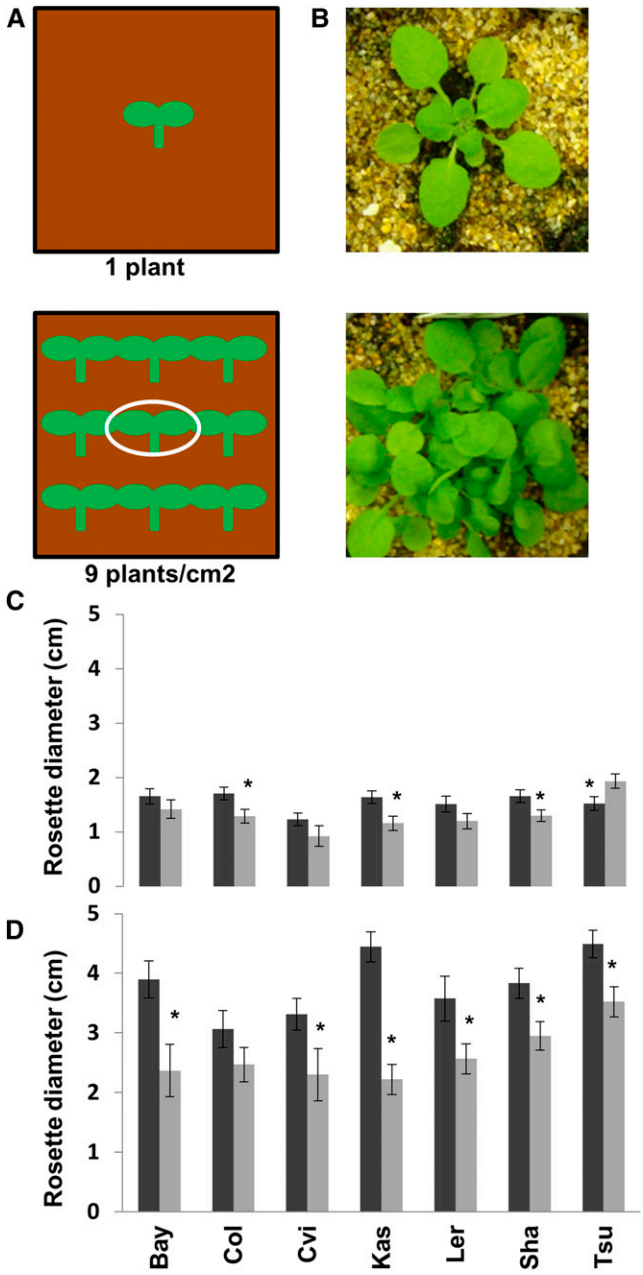

Figure 1. Natural Variation in Response to Competition.

Dark-gray bars represents control growth, and gray bars represent competition. Asterisks indicate significance at $P < 0.05$ using ANOVA with post-hoc Tukey's mean comparison. The full experiment was conducted twice with six replicates per accession per experiment. Error bars show SE.

(A) Schematic representation of the competition experiment where nine plants were planted in 1 cm^2 of soil plots for competition (bottom). The center plant for which the measurements were recorded is circled. A single plant growing alone is used as the control (top).

(B) Photographs of the Tsu accession growing at 3 weeks after planting under control conditions (top) and with competition (bottom).

(C) Rosette diameter of seven Arabidopsis accessions measured at 3 weeks after planting.

(D) Rosette diameter of seven Arabidopsis accessions measured at 4 weeks after planting.

A third key aspect of rhizosphere stimuli that alters root foraging is the availability of nutrients in the local soil that leads to altered root growth to maximize the ability to obtain these nutrients. In general, the plant changes the root growth pattern to optimize the ability to obtain specific nutrients from soil. This can include increasing lateral root growth in the presence of nitrogen or directing the growth of roots toward sources of water (Roycewicz and Malamy, 2012). This can even include altering the root growth pattern in the presence of nutrients not typically considered to be sourced from the rhizosphere, such as carbohydrates (Freixes et al., 2002). While these responses lead to altered partitioning of growth between the root and shoot, the specific mechanisms beyond a nutrient imbalance are not well understood nor is it clear how many rhizosphere stimuli trigger foliar responses. Thus, there is a need to test the ability of unexpected rhizosphere variation to influence foliar growth.

To identify the genetic mechanisms that enable belowground environmental perturbations to influence foliar growth, specifically spatial constraints, we tested if accessions have natural variation in their response to growing in close proximity to a common reference genotype. This showed that there was significant variation in growth in response to a common competitor. To focus on spatial aspects of growth constraints within the soil, we tested if these same accessions were responsive to above- and belowground growth constraints. This showed extensive genetic variation in responses to root and shoot constraints and suggested that these responses were possibly genetically independent. To identify genetic loci that link belowground perturbations with changes in foliar growth, we focused on the variable response to spatial constraints present within the soil. Using an experimental system, where plant roots were grown in rhizosphere tubes of 0.5 cm diameter, we observed natural variation in shoot response to root constraint in *Arabidopsis thaliana*. Using an Arabidopsis recombinant inbred line (RIL) population, we measured changes in plant shoot growth under root constraint to identify genomic loci that regulate the shoot growth and biochemical responses to root constraint. Validation tests showed that natural variation in *EARLY FLOWERING3* (*ELF3*) links the shoot response to root constraint and begins to highlight that root and shoot responses must be coordinated to properly respond to variation in the soil environment. Our analysis reveals a complex genetic regulation of the shoot growth responses to root constraint in Arabidopsis.

RESULTS

Natural Variation in Response to Competition

To begin studying the genetic regulation of plant responses to rhizosphere constraint, we tested for genetic variation in competition responses in Arabidopsis. We compared how Arabidopsis accessions grow in isolation or when nine plants of the same genotype were grown per 1-cm^2 plot to measure the response to crowding (Figures 1A and 1B). At 3 and 4 weeks of age, rosette sizes of the uncrowded plant and solely the plant at the center of the crowding design were measured (Figure 1A). At 3 weeks after planting, the accessions showed statistically significant genotype × treatment interactions ($P = 0.016$) in how the rosette size responded to crowding (Figure 1C). Some accessions (Col, Kas, and Sha) were significantly smaller under crowding compared with the control while

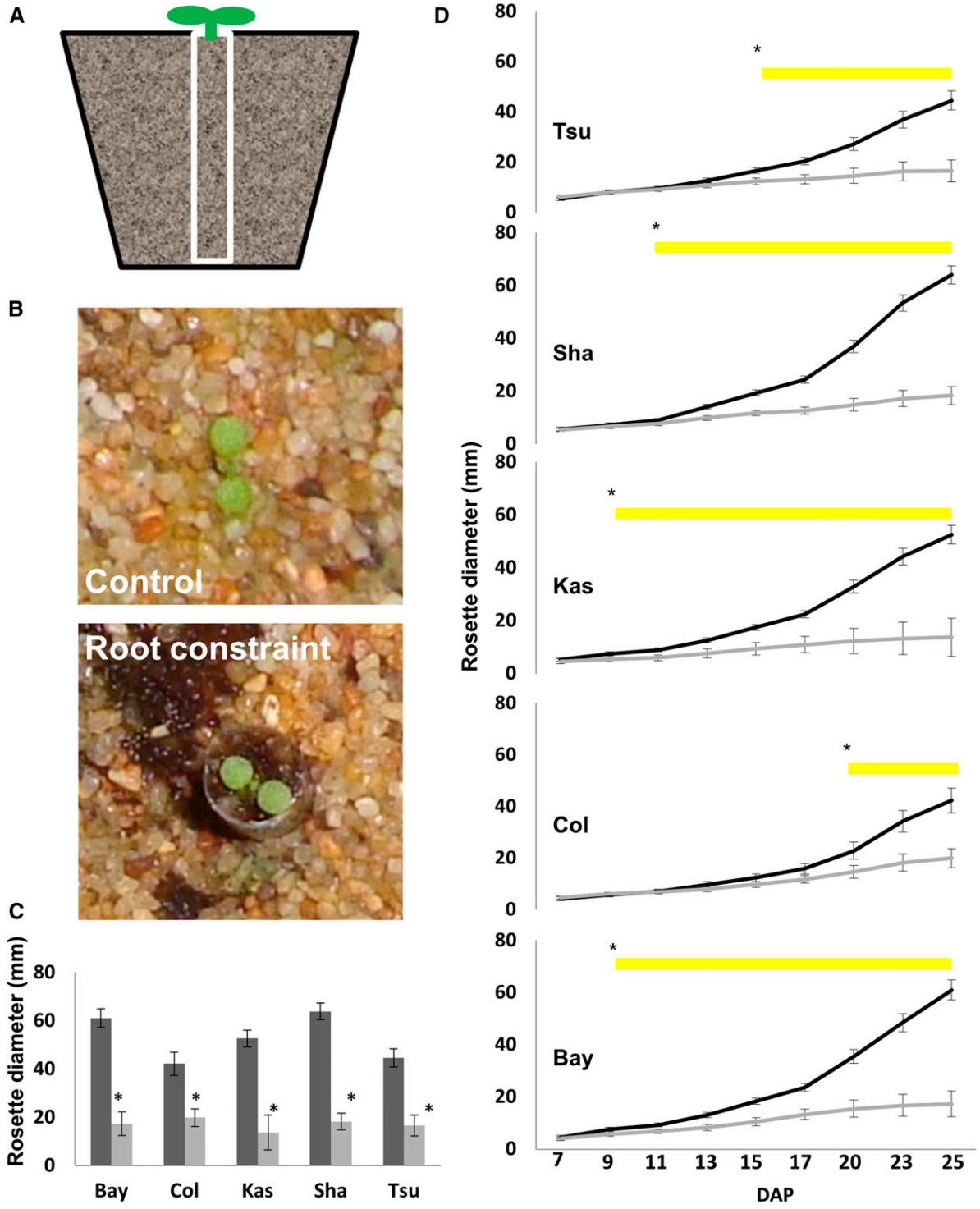

Figure 2. Natural Variation in Response to Root Constraint.

(A) Schematic representation of root constraint showing rhizosphere tubes filled with soil in which the roots were grown. Tubes are 0.5 cm in diameter.
(B) Arabidopsis plants growing under control conditions and root constraint.
(C) Rosette diameter of Arabidopsis accessions at 25 DAP. Dark-gray bars represent control, and gray bars represent root constraint. Asterisks indicate significance at $P < 0.05$ as estimated using ANOVA with post-hoc Tukey's mean comparison. The experiment was conducted twice with nine replicates per accession per experiment. Error bars present SE.

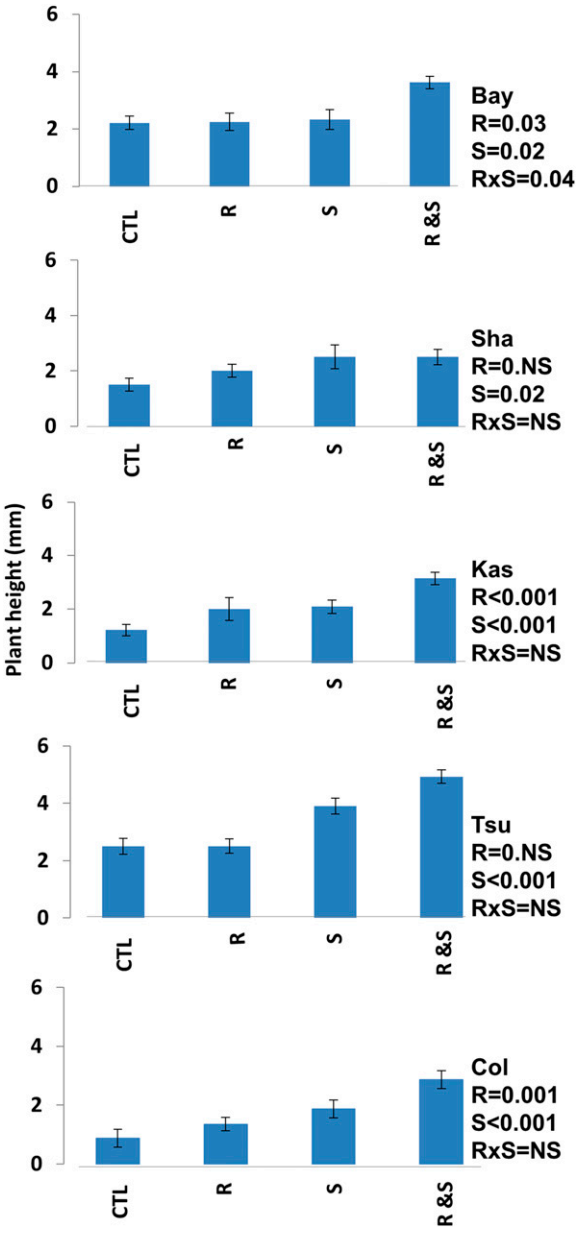

Figure 3. Natural Variation in Response to Above- and Belowground Constraint.

The plant height of five accessions was measured at 4 weeks after planting in the presence of root and/or shoot constraint. The significance P values obtained from the two-way ANOVA for the root (R), shoot (S), or interaction (RxS) constraint on the accession's growth are listed to the right of the graph. Analysis was conducted within each accession using ANOVA, and the accessions are named for each graph. There were nine independent replicates per accession.

others (Bay, Cvi, and L*er*) did not show significant changes in rosette diameter under crowding. By contrast, Tsu showed a beneficial effect of crowding such that the crowded rosette was larger than the uncrowded rosette at 3 weeks. At 4 weeks after planting, all of the accessions except Col showed a significant reduction in rosette size under crowding conditions (Figure 1D). This shows that there is natural variation within Arabidopsis for tolerance to crowding. The differential response of Tsu to crowding indicates that some accessions may transiently overcompensate to outcompete their neighbors. While this suggests that there is variation in how Arabidopsis accessions respond to growth constraints, the source of this constraint being another biological organism greatly complicates our ability to resolve the genetics.

Natural Variation in Response to Root/Shoot Constraint

To better resolve how plants respond to spatial growth constraints, we focused on the physical aspect of the constraint. To investigate the potential role of physical constraints within the rhizosphere, we imposed a physical constraint on lateral root growth using a 0.5-cm-diameter tube that imposes a lateral constraint on growth. We grew five Arabidopsis accessions in containers with a centrally placed soil-filled tube (0.5 cm in diameter) surrounding the root, the tube surrounding solely the rosette, or the tube surrounding both the root and shoot. The soil-filled tube was placed in the soil and a pressure plate used to ensure that the compaction level was equalized throughout the soil. For shoot constraint, the tube was placed above the soil surrounding the seed. We dropped the L*er* and Cvi accessions from further experiments because of the large effect of growth loci (*Erecta* and *CRY2*) in both accessions (Torii et al., 1996; Botto et al., 2003). The seeds were centrally placed on the surface of the soil-filled tube such that, as the plant germinates, the roots will grow into the soil inside the tube and will be spatially constrained (Figures 2A and 2B). All plants were visually inspected to ensure that the root and/or shoot had grown into the tube for the respective treatment.

Because a common response to constraint is altered plant height, such as increased growth of the hypocotyl, we measured rosette height in all samples at 4 weeks after planting. This showed a highly significant response to the constraint that was naturally variable across the accessions. The accessions contrasted in their pattern of responses to growth under root or shoot constraint alone or simultaneous root and shoot constraint (Figure 3). The response in plant height under root and shoot constraint was additive for Kas, Tsu, Col, and Sha, such that both treatments increased height and the double constraint was the additive increase of the two single treatments. However, Bay showed a significant interaction, such that there was only a change in height when both roots and shoots were constrained (Figure 3). These observations suggest that some Arabidopsis responses to root or shoot constraint are possibly

Figure 2. (continued).

(D) Rosette diameter of Arabidopsis accessions at successive time points starting at 7 DAP. Black lines are control, and gray lines are root constriction. Asterisks show the time at which the constrained plants begin to show a significant ($P < 0.05$) reduction in rosette size. The yellow bar shows the duration in which the constrained plants are statistically smaller. Significance was done using ANOVA with post-hoc Tukey's mean comparison. Error bars present SE.

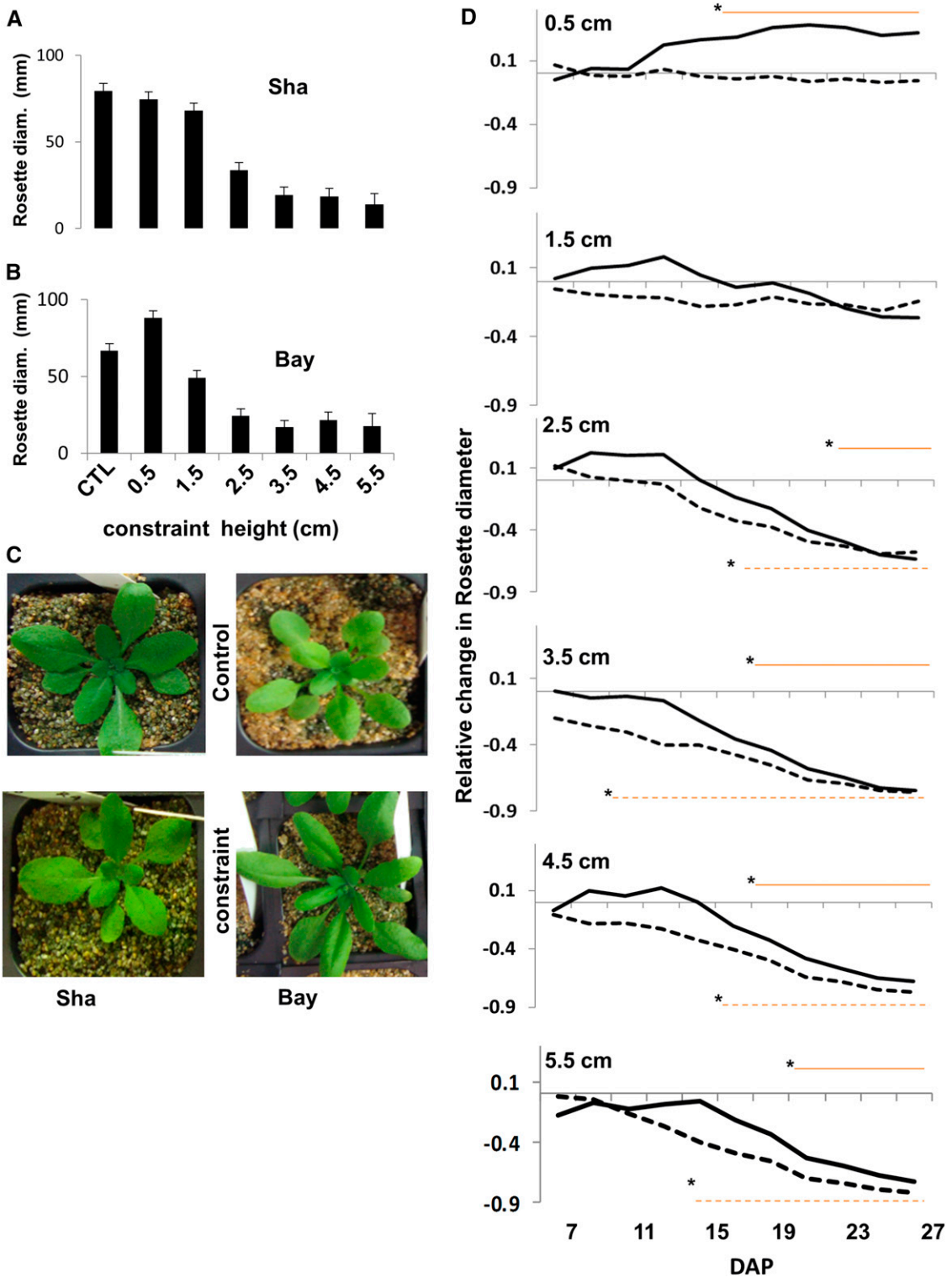

Figure 4. Natural Variation in Response to Various Depths of Root Constraint.

The Bay and Sha accessions were grown in the presence of different depths of root constraint using a 0.5-cm straw and their growth was digitally analyzed every 2 d. Two independent experiments were performed, with six randomized replications per treatment per accession per experiment.

(A) The rosette diameter of Sha measured at 27 DAP across the various depths of root constraint.

(B) The rosette diameter of Bay measured at 27 DAP across various depths of root constraint.

genetically independent, while others integrate between the root and shoot. Thus, natural variation in the responses to root or shoot constraint alone or in combination can be explored to understand the genetic control of these interactions.

Ontogenic Variation of Root Constraint Responses

The Tsu accession showed differential responses to constraint across developmental age, also known as an ontogenic dependency (Figure 1). Thus, we tested if there is variation in the age at which Arabidopsis accessions respond to root constraint (Figure 2C). The accessions showed significant differences in the age at which the accessions exhibited a response in rosette size to the root constraint (Figure 2D). Bay and Kas showed significant reductions in rosette size as early as 9 d after planting (DAP). By contrast, Col showed a significant reduction only from 20 DAP onwards. This apparent variation in the timing appears to coincide with the date at which the accession accelerates its growth rate in the control samples. We also measured flowering time of all the plants in this experiment and there was no significant change in flowering time due to treatment (Supplemental Data Set 1). Thus, the root constraint appears to have a specific impact on growth rate and not on flowering time, suggesting that the response to root constraint initiates a switch that alters the rate of growth without changing general ontogenic development of the plant (Figure 2D; Supplemental Figure 1).

Conditional Response to Root Constraint

To begin identifying potential loci that regulate the differential rosette growth response to root constraint, we focused on the Bay and Sha accessions that are the parents of a well-studied RIL population with significant genomic and transcriptomic resources (Loudet et al., 2003a, 2003b, 2005; West et al., 2006, 2007; Bouteillé et al., 2012). We first tested if restricting the roots' lateral growth along the entire pot depth is too severe a constraint to measure variation between the accessions. Measuring how Bay and Sha respond to different depths of constraint from the soil surface showed significantly different responses to the various depths of root constraint (Figure 4). Constraint limited to the very top 0.5 cm of the roots significantly stimulated the shoot growth of Bay, but had no significant effect on Sha growth (Figure 4). A constraint of 1.5 cm had no effect on either accession, while constraints of 2.5 cm or longer elicited a similar reduction in rosette size irrespective of the depth of constraint in both Bay and Sha (Figures 4A and 4B). This growth reduction always occurred at an earlier ontogenic plant age in Sha in comparison to Bay, showing that the ability to detect the rosettes' response to root constraint in these two accessions is conditional on both plant age and depth of constraint (Figure 4D; Supplemental Figure 2). These consistent genotype-specific responses to root constraint show that there is genetic variation in these two accessions for rosette response to root constraint.

Genetic Regulation of Response to Root Constraint

To map the loci that regulate the variable responses of Bay and Sha to root constraint, we undertook quantitative trait loci (QTL) mapping using the Bay × Sha RIL population (Loudet et al., 2002). We grew 211 lines of this population within a 0.5-cm-deep root constraint or control conditions and digitally measured the rosette sizes at consecutive days starting at 7 DAP and shoot fresh weight at 35 DAP. We focused on the 0.5-cm root constraint, as this is the weakest treatment, suggesting that it should have the fewest indirect physiological effects, and as it also had a positive growth effect on the Bay accession. Furthermore, previous research has shown that the Bay and Sha parents and RILs have a root growth rate that would allow the seedlings' roots to grow below this constraint barrier within 24 h of germination (Loudet et al., 2005; Bouteillé et al., 2012; Kellermeier et al., 2013). Additionally, the soil within this constraint was packed to the same level as the surrounding soil and the constraint did not restrict the flow of water or oxygen given the surface-to-volume ratio. To equilibrate soil compaction within and outside of the straw, we placed the straw vertically in the total soil of the pot and placed equal pressure across the total surface area of the pot. The specific mechanism of this response to a 5-mm-deep root constraint will require detailed further investigation. Of particular interest is finding the genes controlling this response.

Across the population, the average growth under constraint tended to be higher than that found under the control conditions (Supplemental Figure 3 and Supplemental Data Set 2). Linear modeling to partition the phenotypic variation showed that there were significant effects of genotype and genotype × treatment on all growth phenotypes. The broad-sense heritability for the RILs for genotype alone ranged from 31 to 45% across the different days that rosette size was measured with an average heritability of 37% (Supplemental Figure 4A and Supplemental Table 1). Genotype and genotype × treatment interactions together accounted for the major share of the total variation (50 to 57%), with an increasing trend toward the later days of growth. Additionally, the distribution of rosette sizes across the population showed that the growth phenotypes are likely highly polygenic (Supplemental Table 2 and Supplemental Figure 3).

QTL Analysis

Using the above linear model, we obtained the model corrected least square means for all growth traits for each RIL under each treatment condition (control and 0.5-cm constraint). Because of seedling mortality, we had complete data for 194 RILs in the

Figure 4. (continued).

(C) Image of Bay (right) and Sha (left) rosettes under control and root constraint conditions, indicating the shoot growth stimulation of Bay under constraint.
(D) Relative change in rosette diameter of Bay and Sha compared with control as growth progresses under increasing depths of root constraint. Solid lines show the size of Bay and dotted lines indicate the size of Sha. Asterisks indicate the time point when a statistically significant ($P < 0.05$) deviation from control begins for each genotype using ANOVA. The top of the graph and orange line show the time points at which Bay has a response to the restriction for each depth of root constraint. The bottom of each graph and dashed orange line shows the time points at which Sha has a significant response to root constraint.

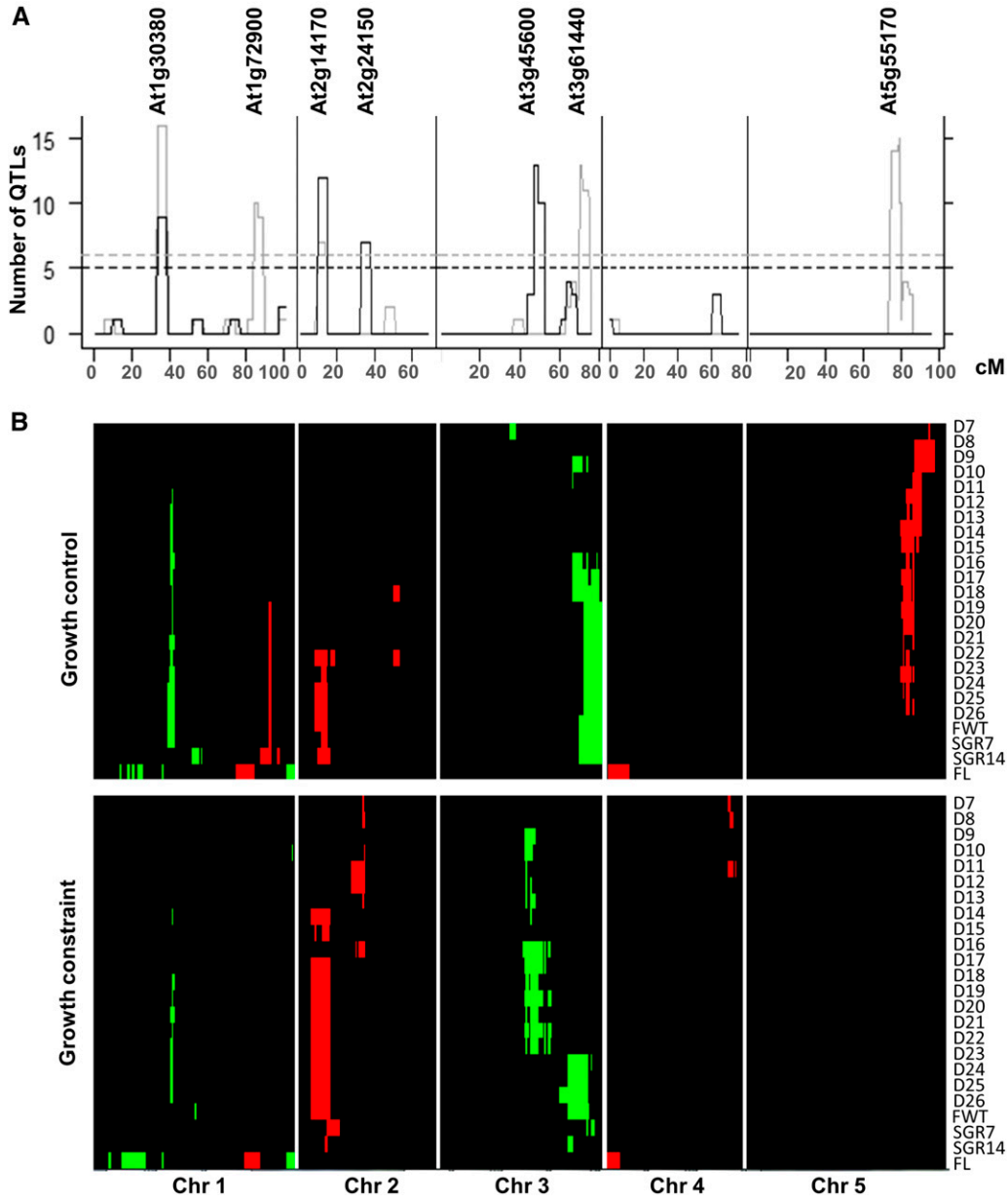

Figure 5. Genomic Architecture of QTLs Associated with Growth Traits.

QTLs were mapped for all growth and flowering time traits using the Bay × Sha RIL population

(A) QTLs associated with growth under control and root constraint conditions are shown. The number of QTLs associated with growth within a 5-cM window of the genome is plotted against the genetic location in cM. QTL hot spots for growth phenotypes under control conditions are shown in gray and in the presence of a 0.5-cm-deep constraint in black. The horizontal dashed lines represent the permuted threshold (P = 0.05, 1000 permutations) for significant hot spots. Hot spots are labeled above the respective locus with representative markers that is closest to the peak.

(B) A heat map showing the location and effect of significant loci detected for all growth and flowering time traits across the five chromosomes. Red indicates a positive effect of the Sha allele, while green indicates a positive effect of the Bay allele. Vertical white lines separate the chromosomes (1 to 5 from left to right). Heat map for growth in control conditions (top) and under 0.5-cm-deep root constraint (bottom), with rows corresponding to each growth phenotype as labeled on the right. The phenotypes are abbreviated such that D7 to D26 indicate the rosette size from 7 to 26 DAP. FWT is the weight of the plants at day 26, SGR is size standardized growth rate for the indicated interval, and FL is flowering time.

control data set and 198 RILs in the constraint data set for QTL mapping. Using a total of 24 growth phenotypes for each treatment condition, we identified 74 QTLs affecting growth in the control plants and 58 QTLs identified for the constricted plants. On average, this was 3.1 QTLs per growth phenotype for control plants versus 2.3 QTLs per phenotype under root constraint.

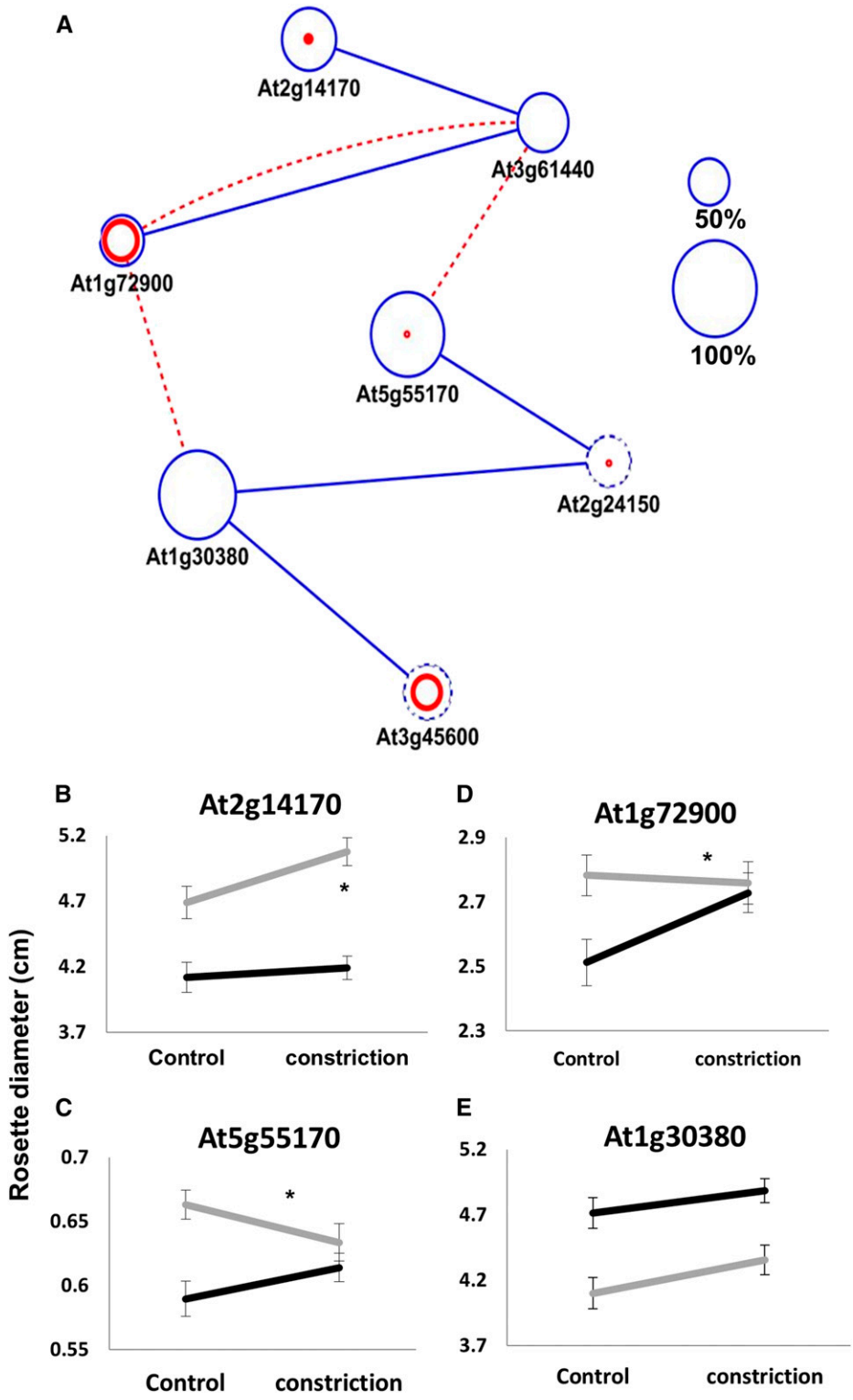

Figure 6. Epistatic Interactions and QTL × Treatment Interactions That Regulate Growth under Constraint.

(A) Network showing statistically significant QTL × QTL interactions for the seven QTL hot spots. Blue nodes represent each of the seven QTL hot spots with the size of each node representing the fraction of growth phenotypes showing a significant main effect at that locus. The dotted blue nodes show genetic loci that were detected as being significant in the presence of the 0.5-cm-deep root constraint. The red circles and dots within each node indicate loci that show

A sliding window analysis of the number of QTLs across the genome to identify significant QTL clusters revealed five significant clusters for growth of control plants and four significant clusters under root constraint (Figure 5A). A majority of these QTL clusters appeared specific for each condition; two clusters specific to root constraint and three clusters specific to control. The two QTL clusters specific to growth under root constraint showed opposite allele effects, with the QTL cluster on Chromosome 2 increasing growth with Sha allele, while the cluster on Chromosome 3 increases growth with the Bay allele (Figure 5). Thus, both Bay and Sha have alleles that allow for increased rosette size in response to a shallow root constraint, even though only the Bay parent showed a response.

In agreement with the previous observation of ontogenic-dependent variation between the parents, we found that the QTL appeared to have age-limited effects. For example, the QTL cluster at the top of Chromosome 2 only affects growth as measured in older plants (Figure 5B). An example of a QTL cluster that displays differences between the treatments is the cluster located in the middle of Chromosome 3 and only significantly affected plant growth under root constraint (Figure 5B). There were also QTL clusters that were both age and condition specific, such as the one in the middle of Chromosome 2 that only appeared in young plants that were root constrained (Figure 6B).

In our control experiments, the Bay parent showed increased growth under the 0.5-cm root constraint, whereas the Sha parent had no difference in growth under the two conditions. In agreement with this, the Sha allele increases growth for more than half of the QTLs detected under control conditions, whereas the Bay allele increases growth for the majority of QTL detected under root constraint (Figure 5). However, this was not uniformly the case, as there were QTLs where the Sha allele provided increased growth under root constraint conditions and the Bay allele functioned under control conditions. Thus, there is transgressive segregation in the RIL population for the growth effect of root constraint. Thus, the variation found in the parents is not a complete representation of the genetic potential of this phenotype. Even though the Bay parent alone showed stimulated growth under root constraint, our QTL analysis indicated that both Bay and Sha alleles have growth stimulating effects.

Flowering Time Variation

In addition to growth, we also measured flowering time in all the RIL plants in both conditions. The linear model showed no significant effect of the root constraint treatment on flowering time nor any effect on the interaction of RILs with treatment (Supplemental Table 1). In agreement with this, all QTLs detected for flowering time were found in both treatment conditions (Figure 5B). Several of the detected flowering time QTLs localize to known flowering loci segregating in this population (e.g., *FRIGIDA* and *FLOWERING LOCUS C*) (Michaels and Amasino, 1999; Johanson et al., 2000). Furthermore, none of the QTLs for flowering time overlapped with any of the growth QTLs (Figure 5B). This lack of root constraint effect upon flowering time suggests that the effect of root constraint on rosette growth does not have global effects on the flowering time transition. The lack of any overlap in growth or flowering time QTLs also suggests that variation in flowering and growth in this population may not be causally linked.

QTL × Treatment Interactions

One complication of QTL analysis is that if there is a sufficiently high number of causal loci for a trait there is the potential for false positive/negative error rates to increase (Beavis, 1994, 1998; Bernardo, 2004; Joseph et al., 2013). Thus, we wanted to directly assess if there were significant QTL × treatment interactions using a linear model rather than solely rely on QTL overlap to infer treatment interactions. Using the QTL clusters that regulate growth variation under control and constraint conditions, we identified a genetic marker at the center of each cluster to use as a genetic term in a single multi-QTL linear model. Markers are named by the closest gene to provide ready interpretability, but this is not intended to claim any causality for that gene. This allows us to specifically test all loci within a single linear model. Within this model, we used all the mean growth data for each RIL under each treatment and included treatment as a factor in the model to allow us to directly test the QTL × treatment interactions. All seven QTL clusters had significant main effects, with the fraction of phenotypes significantly affected by the clusters ranging from 54 to 92% (Figure 6; Supplemental Data Set 3). The main effect of all QTL clusters were modulated by plant age with some of the QTL clusters significantly affecting only early growth while others limited to late age growth. These patterns were in agreement with the QTL detection in early versus late growth stages (Figure 6). In addition to the significant main effects, five of the seven QTL clusters showed significant treatment interactions with an array of responses to root constraint (Figures 6A to 6D). Even though all the hot spots appeared to be treatment conditional in the QTL mapping, there were loci that showed no significant treatment effect in the linear modeling, suggesting that the hot spot overlap approach overestimated the treatment × genotype interaction (Figure 6E). Extending the analysis showed that treatment interaction was even dependent on plant age, as shown by the At3g45600 cluster where the G × E significance increased as the plants aged (Supplemental Data Set 4). Thus, while

Figure 6. (continued).

a significant genotype × treatment interaction using ANOVA. The size of the red circle represents the fraction of growth phenotypes showing a significant treatment interaction at each locus. Blue edges connect loci that show significant QTL × QTL epistasis. Red dashed edges connect loci that show significant conditional epistatic interactions, i.e., QTL × QTL × treatment interactions.

(B) to **(E)** The allelic effect of representative QTL hot spots under control and 0.5-cm-deep root constraint growth conditions is shown to illustrate the different patterns of genotype by treatment interactions at each locus. Rosette diameter at representative days is given, with black lines showing the average growth of RILs with the Bay alleles and gray lines showing the average growth of RILs with the Sha allele. **(B)** and **(E)** show data from 22 DAP, **(C)** is from 9 DAP, and **(E)** is from 22 DAP. These are the ages with the maximal effect for the specific loci. Error bars show SE. Asterisks show that there was a statistically significant QTL × treatment interaction using a two-way ANOVA.

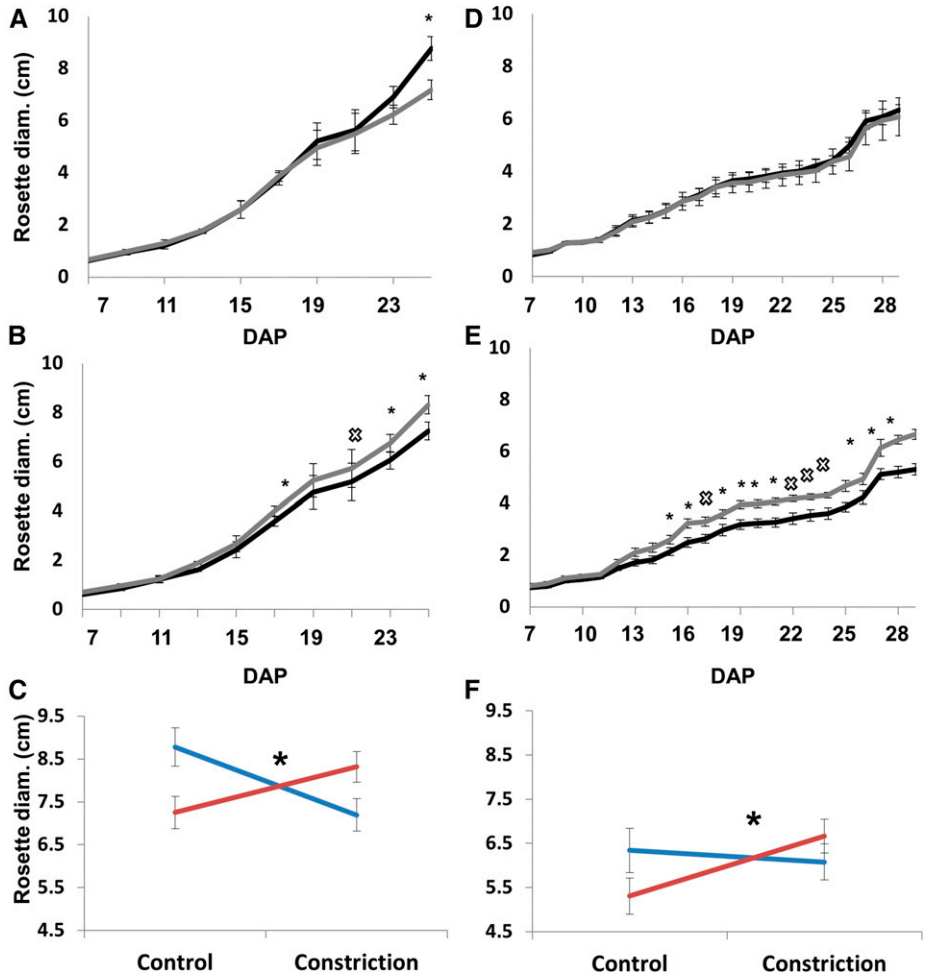

Figure 7. QTL Validation.

An analysis of the rosette diameter of two HIFs that overlapped two QTL hot spots on chromosome 2. Black lines represent growth under control conditions, and gray shows growth under 0.5-cm-deep root constraint. Error bars represent standard errors. Asterisks represent significance at $P < 0.05$, and a cross represents significance at $P < 0.1$ using ANOVA. For each comparison, there were two independent experiments with six randomized replicates for each treatment × genotype combination. Asterisks show a P value of < 0.05, and crosses show a P value of < 0.10 for an interaction of genotype × treatment using a two-way ANOVA.

(A) Rosette diameter of the Bay allele of HIF364 (QTL, At2g14170).

(B) Rosette diameter of the Sha allele of HIF364 (QTL, At2g14170).

(C) Rosette diameter at 26 DAP of HIF 364 Bay and Sha under control and constraint conditions. Blue line is for Bay and red line is for Sha. The asterisk shows that there is a significant allele × treatment interaction using ANOVA ($P < 0.05$).

(D) Rosette diameter of the Bay allele of HIF163 (QTL, At2g24150/ELF3).

(E) Rosette diameter of the Sha allele of HIF163 (QTL, At2g24150/ELF3).

(F) Rosette diameter at 29DAP of HIF 163 Bay and Sha under control and constraint conditions. Blue is for Bay and red is for Sha. The asterisk shows that there is a significant allele × treatment interaction using ANOVA ($P < 0.05$).

the direct QTL mapping made the loci appear specific to either the control or root constraint conditions, all the loci had significant main effects and only a subset had significant G × E interactions.

Epistasis (GxG) and Conditional Epistasis (GxGxE)

We extended the above multi-QTL linear model to test for epistatic interaction between the QTL clusters. Within this model, we used all the mean growth data for each RIL under each treatment and included treatment as a term in the model to allow us to test for both QTL × QTL interactions as well as QTL × QTL × treatment interactions. Using simply the genotype × genotype epistatic tests between QTLs, we identified two epistatic interaction networks among the QTLs (Figure 6, blue solid edges): one connected four loci and another connected three loci. Extending this analysis to directly test if the epistatic interactions were dependent on the root constraint identified interactions between four loci that were conditional on the treatment. These interactions involved two

genes in each of the main effect epistatic networks, thus connecting these sub networks (Figure 6A, red dashed edges). Interestingly, two of the loci showing significant QTL × QTL × treatment interactions had no QTL × treatment interaction (At1g30380 and At3g61440). Thus, it is possible to identify treatment conditional epistasis affecting root constraint, and together this characterizes all the identified QTLs as part of a single genetic network that regulates a plant's response to root competition.

HIF and ELF3 Validation

To validate the QTLs, we used heterogeneous inbred families (HIFs) that segregated for the QTL regions (http://publiclines.versailles.inra.fr/) (Loudet et al., 2002; Bouteillé et al., 2012). We used two different HIFs that segregated for the two QTLs on Chromosome2; HIF364 segregates for the At2g14170 QTL and HIF163 segregates for the At2g24150 QTL. Testing the rosette growth of HIF lines with the Bay or Sha allele at the QTL region under root constraint confirmed the QTL effects. The Bay-0 allele of HIF364 had a negative rosette size response to root constraint, while the Sha allele had a positive response with this HIF, showing a significant genotype × treatment effect (Figures 7A, 7B, and 7E). HIF163 lines had a significant genotype × treatment effect and the Sha allele also showed larger rosette sizes under root constraint, in agreement with the QTL effects, while the Bay allele largely showed no response (Figures 7C, 7D, and 7F). This shows that we are able to identify loci that regulate differential rosette growth responses to root constraint in this RIL population.

The segregating region in HIF163 contains natural variation in *ELF3*, which was previously identified as a regulator of natural variation in the shade avoidance syndrome (Jiménez-Gómez et al., 2010; Jimenez-Gomez et al., 2011). The borders of this HIF have not been fully resolved, but cover at least ~2 Mb from MSAT2.7 to MSAT2.41 or ~500 genes. To test if *ELF3* regulates growth responses to root constraint, we used previously available *ELF3* quantitative complementation lines wherein the Bay or Sha *ELF3* allele is present in an *elf3* mutant background (Jiménez-Gómez et al., 2010; Jimenez-Gomez et al., 2011). The *ELF3* quantitative complementation lines show significantly different responses to root constraint (Figure 8). A nested ANOVA showed no significant differences between the two independent transgenic lines for each *ELF3* allele, suggesting that the observed effects are due to the alleles and not the specific integration event. However, the use of only two independent transgenic lines means that we do not have significant precision in estimating the effect of the difference between the *ELF3* alleles. Interestingly, the rosettes of lines containing the *ELF3* Bay allele are largely nonresponsive to root constraint, while the Sha allele shows a decrease in growth (Figure 8). This validates that *ELF3* is a gene containing causal variation that alters the rosette growth response under root constraint. Interestingly, while the *ELF3* locus is within the HIF163 region, the *ELF3* alleles do not phenocopy the HIF163 response to root constraint. This suggests that there must be causal loci within the HIF163 region in addition to ELF3 potentially with opposing effects.

DISCUSSION

It is well established that plant roots modify their developmental programs according to the prevailing soil conditions (Hodge, 2004; Cahill et al., 2010; Nord et al., 2011).This includes the monitoring of the soil conditions for fluctuations in nutrient availability, physical obstacles, and other aspects with ensuing changes in root growth to allow for proliferation in areas that are most favorable (Semchenko et al., 2008). The root's responses to the environment also have the capacity to generate signals that can alter the growth and development of the shoot. However, there is a lack of understanding of how roots perceive their physical environment or how these responses are regulated at the genetic or molecular level. To begin to gain a mechanistic understanding of these complex responses, we used natural variation of Arabidopsis shoot growth responses to root spatial constraint. The natural accessions differed in their response to root constraint via a mechanism that seemed to be linked largely to the timing of growth adjustments with the more tolerant accessions taking longer to respond to the constraint (Figure 2). Interestingly, some accessions perceived root and shoot constraints via an additive process while others responded in a rather integrative manner, suggesting that these signals or the downstream events are integrated differently in different accessions (Figure 3). The varied shoot responses of these accessions in response to root and shoot constraint suggest that there could be direct signals to regulate shoot growth in addition to indirect consequences of root allocation under root constraint. Our analysis of plant height under shoot/root constraint (Figure 3) and recent reports showing that root and shoot competition interact (Gersani et al., 1998; Falik et al., 2003; Lankinen, 2008) support this possibility.

To dissect how the plant may be responding to the root constraint, we exposed two accessions that differ in their susceptibility to root constraint, Bay and Sha, to varying depths of constraint. Sha was largely unresponsive to root constraint until ~2.5 cm with the shift from no response to response being nonlinear. By contrast, Bay showed an unexpected stimulation in shoot growth at the 0.5 cm constraint depth followed by diminished growth rates at 2.5 cm and deeper (Figure 4D). Interestingly, Sha, which was originally classified as an accession not responding to root constraint, responded more quickly than Bay with diminished growth. Sha displayed diminished growth four days earlier than the Bay accession (Figure 4D). This suggests that there is natural variation both in the sensitivity to root constraint and the timing of the shoot's response to this constraint. Thus, exploring the natural genetic variation could be a valuable tool in efforts to dissect how the plant coordinates its root and shoot responses to root challenges and to establish if this coordination varies by the type of challenge (Fang et al., 2013).

Complex Genetics of Natural Variation under Root Constraint

To dissect the genetics underlying these differential responses to root constraint, we mapped rosette growth QTLs in the Bay × Sha RIL population in the presence and absence of a 0.5-cm depth of root constraint that stimulated Bay growth and generated no change in Sha growth. Nondestructive digital imaging allowed us to measure rosette growth in real time and map QTL that were dependent on the rosette constraint and the plant's age. This showed that the genetic control of rosette growth was highly polygenic, with the majority of loci being conditional to the plant's

age or the root constraint (Figure 6). Comparing our results to previous assays of root architecture in the Bay × Sha population identified only a single locus that overlapped, suggesting that the loci we are finding are not solely root architecture loci (Loudet et al., 2005). Testing for epistasis between identified loci showed that there were numerous interactions and that these were conditional upon the plant age and root constraint (Figure 6). The ability to identify genetic interactions among these loci suggests that they may function in a connected network and that this network is highly conditioned by the age and condition of the plant. It remains to be tested how frequently plant age (ontogeny) interacts with natural variation in an environment-dependent fashion (Wentzell et al., 2008; Wentzell and Kliebenstein, 2008; Edwards et al., 2012). This does show that any molecular genetic studies of root-shoot communication in Arabidopsis need to consider the age and conditions of the plant when working to extrapolate the observations.

ELF3: A Link between Shoot Responses to Above- and Belowground Signals?

One of the QTL regions showing a genotype × root constraint interaction in our study overlapped with the previously cloned *ELF3* genomic region (Figure 8). Natural variation at this locus in this population has been shown to alter the rosette's shade avoidance response as well as flowering time and defense chemistry (Jiménez-Gómez et al., 2010; Jimenez-Gomez et al., 2011). However, the flowering time effects were only identified under different conditions from the ones we used (Jiménez-Gómez et al., 2010; Jimenez-Gomez et al., 2011). Using the quantitative complementation lines from this study allowed us to show that natural variation between the Bay and Sha *ELF3* alleles also alters how the plant's rosette responds to root constraint. The Bay allele of *ELF3* is unresponsive to a 0.5-cm-deep root constraint, while the Sha allele of *ELF3* leads to diminished growth under the same conditions. Thus, it appears that *ELF3* can link the root's environment to alterations in shoot growth. Given the shallow 5-mm-deep root constraint, it is unlikely that this ELF3-mediated response is caused by altered oxygen or water availability, as the surface area is sufficient to allow for proper diffusion. It is possible that *ELF3* integrates root and shoot signals during competition to regulate the circadian clock and to elicit growth responses (Covington et al., 2001; Hicks et al., 2001; Liu et al., 2001; Nieto et al., 2015). The Bay and Sha *ELF3* alleles vary in the length of a poly-glutamine stretch and have an Ala (Bay) to Val (Sha) transition that leads to altered localization and posttranscriptional regulation via unknown mechanisms (Undurraga et al., 2012; Anwer et al., 2014). Future work will be required to determine how *ELF3* mediates the flow of information between the root and shoot and to identify the signal that mediates this interaction.

Comparing the results of the *ELF3* complementation lines with the HIF for this region (HIF163) provided evidence that the QTL near *ELF3* is likely polygenic in nature. HIF163 shows contrasting responses in rosette growth in the presence and absence of a 0.5-cm-deep root constraint (Figure 7) in agreement with the original QTL (Figure 5). By contrast, the *ELF3* quantitative complementation lines only displayed an effect under constraint. Thus, this QTL region likely contains other loci that also affect the rosette's growth response to root constraint. This suggests that our population of 211 lines is not sufficient to separate the effects of these loci as well as the possible genetic interactions. Therefore, it is likely that the loci we uncovered in this study are only a subset of all the loci that regulate the rosette's response to root constraint.

What Rhizosphere Element Does the Lateral Root Constraint Alter?

While our results show that Arabidopsis accessions have the ability to detect a shallow 5-mm-deep root constraint and alter rosette growth, the specific mechanistic basis behind this change is difficult to define, especially given the difficulty of visualizing the roots in these conditions. One option is that the root growth angle away from the gravity vector may lead one accession to perceive the physical barrier more than another. However, given that the root constraint is 5 mm deep × 5 mm in diameter, this would require a root angle of 26.6 to hit the very bottom of the physical barrier. In agar, the Bay accession has been found to have a root growth angle of only 2 degrees off of vertical and only 1 of 163 accessions had an angle of greater than 19 degrees off of vertical (Slovak et al., 2014). Thus, this is likely not a source of difference between the Bay and Sha parents for the 5-mm-deep root constraint. The angle required to hit the barrier at least once decreases to only 9 degrees off of vertical for the 15-mm root constraint, suggesting that thigmotropic aspects may become an issue with the deeper root constraints (Slovak et al., 2014).

Another concern with the lateral root constraints is that they may be limiting water or some other nutrient's availability. We ensured equal compaction and did not saturate the soil to ensure the presence of airspaces that should allow for oxygen penetration, especially for the 5-mm-deep root constraint. Similarly, given the shallow 5-mm-deep root constraint and the fact that the root should pass through this space within 24 to 48 h after germination, the low water use of a seedling should ensure that the surface area available for vertical water and nutrient availability would limit any deficiency. Once the root has passed through this 5-mm constraint, the seedling would rely on the growing primary and lateral roots for nutrient and water foraging and this section of the root would function predominantly as a conduit. However, nutrient or water deprivation is definitely a potential influence with the deeper constraints.

One aspect that the shallow lateral constraint may influence is the lateral diffusion of exudate from the germinating root itself. This could lead to elevated local levels of these compounds and might influence either the plants own signal/perception mechanisms or alter the local microbial population in a way that did not occur in the control treatment. The barriers themselves were flushed to prevent the introduction of chemicals from the barrier itself for this reason. Differentiating between these possibilities will require extensive future genomic and transcriptomic assays to fully assess what plant-perceived signals are altered by the shallow lateral root constraint.

Another noted complication of interpreting these results is that if the root has grown out of the barrier within 24 to 48 h, then how are there growth effects that occur later in development? This could have a number of explanations. First, it is already known that early life history at the embryo stage can influence auxin signaling and

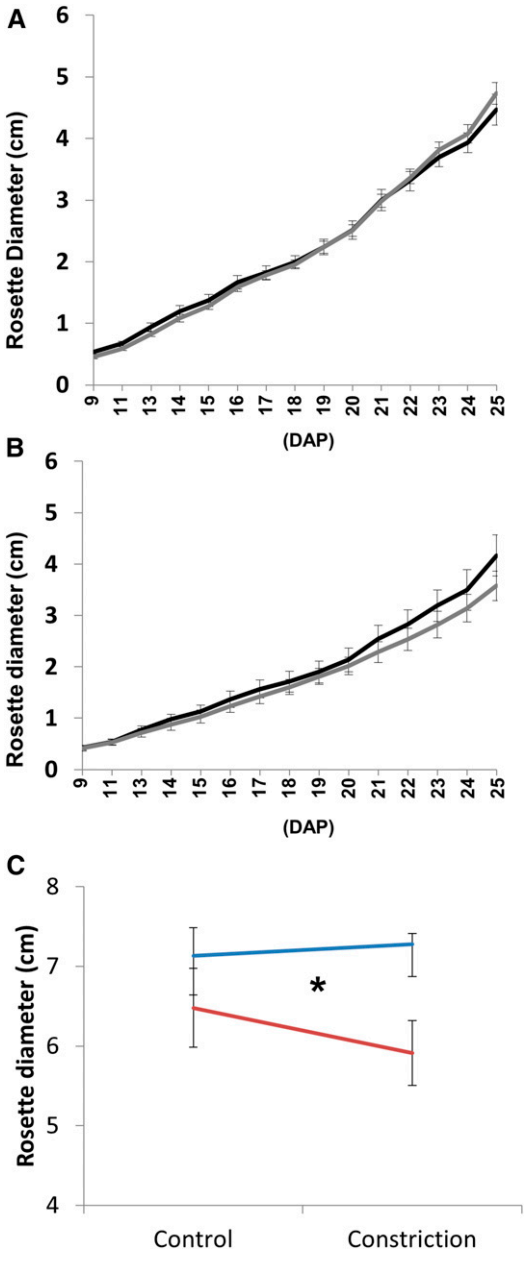

Figure 8. Validation of *ELF3* Variation Influencing Shoot Growth under Root Constraint.

The growth response of homozygous *ELF3* complementation lines to root constraint is shown. For each graph, the daily measured rosette diameter of the homozygous T3 lines is presented. Two independent T3 complementation lines were used for each of the Bay and Sha alleles. There were four independent randomized replicates per genotype. There was no significant variation between the T3 complementation lines for each allele, with black lines representing growth under control conditions and gray showing growth under for 0.5-cm-deep root constraint. Error bars represent standard errors.
(A) Rosette diameter of ELF3 Bay allele complementation lines.
(B) Rosette diameter of ELF3 Sha allele complementation lines under control and root constraint.
(C) Rosette diameter at 33 DAP of ELF3 Bay (blue) and Sha (red) complementation lines under control and constraint conditions. The asterisk indicates that there is a significant genotype × treatment interaction for average rosette size using ANOVA ($P < 0.05$).

ultimately result in differential growth and biomass accumulation (Paul-Victor et al., 2010; Elwell et al., 2011). As growth is an iterative process built on all events that occurred before a given time point, any early life event has the potential to influence the organism even after the event has passed. This process could occur via epigenetic or nonepigenetic processes. Furthermore, if the lateral root barrier has altered the local microbial population, the effect of the barrier may be continuous throughout development. Further studies are needed to differentiate between these options or others not yet considered.

Conclusions

There is increasing evidence that plants detect and respond to changes in their root environment through mechanisms that do not involve changes in resource availability. These mechanisms include touch perception of neighbors' roots or physical obstacles belowground. In our study, we found numerous loci that regulate the ability of the rosette to respond to changes in the root environment, with one of them being ELF3, a key component of the foliar circadian clock. ELF3 is only an entry into this genetic diversity, as there are a large number of other loci that, upon their cloning, could begin to provide insight into how the root and shoot communicate to coordinate the plant's growth. Future studies, including genome-wide association mapping of these responses, will aid our understanding of these processes.

METHODS

Competition Experiments

To test for differential responses to crowding, seven *Arabidopsis thaliana* accessions (Bay, Col, Cvi, Kas, Ler, Sha, and Tsu) were each grown in the center of a 1-cm square with eight siblings planted along the perimeter, giving a planting density of nine plants per cm^2. Each accession grown alone without neighbors served as the control. These accessions were chosen as they are the parents of existing RIL populations with extensive genomic data. Prior to planting, seeds were imbibed in water and cold treated at 4°C for 4 d. Seeds were planted in plastic flats with 36 cells per flat filled with standard potting mix (Sunshine Mix #1; Sun Gro Horticulture) and covered with a thin layer of sand. Each accession was replicated six times per treatment, and the placement of each accession/ treatment was completely randomized within each flat. The full experiment was independently replicated twice providing at least 10 measurements per accession per treatment per week of harvest. Plants were grown in controlled environment growth rooms at 20°C and 16-h/8-h light/dark cycles. Plants were watered with nutrient water staring at 2 weeks after planting to avoid any nutrient and water stress. At 3 and 4 weeks after planting, rosette diameter was measured for the control plant and the center plant in the competition treatment for each accession. For the crowding treatment, replications with fewer than seven neighbors were excluded from the analysis. Different sets of plants were used for growth measurements at 3 and 4 weeks after planting because leaf samples were collected for secondary metabolite analysis at those time points. The rosette diameter and glucosinolate data were analyzed by mixed model ANOVA, where the accession, treatment, and accession and treatment interaction were

included as the fixed terms and experiment as a random effect. The least square means from the above model was used for comparing the accession performance under crowding.

Root Constraint Experiments

For the constraint treatment, roots were grown in 0.5-cm-diameter tubes (Dixie brand translucent plastic straws) that spanned the entire height of the container from the soil surface to the bottom. The containers were filled with soil to the top and covered with a thin layer of sand. The tubes were filled with soil and presoaked to ensure sufficient moisture in the soil within the tubes, prior to inserting into the center of the container filled with soil. The same soil was used in the tubes and the container. Seeds were cold treated for 4 d and planted at the center of the soil in the tube such that the roots will grow into the tube and will be constrained. This was visually confirmed on all seedlings. Plants were watered with nutrient water as described above to ensure sufficient moisture and nutrients. Plants grown without the constraint were used as control. Each flat was digitally imaged every day, starting from 7 DAP. Excess plants were removed prior to imaging and the images were used to measure the rosette sizes using ImageJ image analysis software. Two fully independent experiments were conducted with each experiment having nine randomized replications per treatment/accession. This provided 18 measurements per treatment per accession.

For experiments with varying levels of root constraint, tubes to different depths (0.5, 1.5, 2.5, 3.5, 4.5, and 5.5 cm) were used. Tubes were inserted at the center of the container and were flush with the top of the container so that roots were constrained at varying depths from the soil surface. Rosettes were imaged daily beginning 7 DAP. Two completely independent experiments were performed with six randomized replications per treatment/accession within each experiment. This provided 12 measurements per accession per root constraint depth. Model corrected least square means as described above were used for comparing the accession performance under root constraint.

Growth of Bay × Sha RIL Population

Seeds of the 211 lines of the Bay × Sha recombinant inbred population were grown in a completely randomized design per RIL/treatment. The treatment was either growing with a 0.5-cm root constraint or control without constraint. The entire experiment was repeated consecutively three times in the same climate controlled chamber (20°C and 16-h/8-h light/dark cycles) with independent randomization per experiment. Plants were grown as described above for the root constraint experiments. The full population required eight planting flats, which we treated as a block term within the ensuing linear model. Plants were imaged daily from 7 DAP and rosette diameter was measured from the images. At 35 DAP, shoots were removed and fresh weight was measured. Flowering time was measured as number of days until first flower opened for all the RILs that flowered by 35 DAP. Size standardized growth rates (SGRs) for each RIL were estimated from daily rosette sizes as described previously (Paul-Victor et al., 2010; Züst et al., 2011; Joseph et al., 2013). This was conducted twice using either the 7 or 14 DAP rosette size as the baseline reference.

Estimation of Heritability

All phenotypic data from three independent experiments with one replication for each treatment per experiment were used to calculate estimates of broad-sense heritability (H) for each phenotype as $H = \sigma^2_g/\sigma^2_p$, where σ^2_g was the estimated variance for RIL genotypes and σ^2_p was the total phenotypic variance for a trait (Liu, 1998). The ANOVA model (line heritability model) for each metabolite phenotype in each line (y_{gte}) was: $y_{gte} = \mu + G_g + T_t + E_e + G_g \times T_t + G_g \times E_e + T_t \times E_e + \varepsilon_{gte}$, where; g = 1…211 RILs, t = treatments: control or root constraint, E = experiment 1…3.The proportion of variance partitioned to the G term was used to estimate the broad-sense heritability. The model was also used to provide model corrected least square means for ensuing QTL mapping.

QTL Analysis

A genetic map comprising of 568 markers was previously available for the Bay × Sha RIL population (Loudet et al., 2002). The least square means of 24 growth phenotypes, including daily rosette sizes, shoot fresh weight, flowering time, and SGR in the presence and absence of root constraint, were used for QTL analysis. For QTL detection, composite interval mapping was implemented using cim function in the R/qtl package with a 10-centimorgan (cM) window. Forward regression was used to identify three cofactors per trait. The declaration of statistically significant QTLs was based on permutation-derived empirical thresholds using 1000 permutations for each mapped trait. QTLs with a LOD score of above 2 were considered significant for further analysis (Churchill and Doerge, 1994; Doerge and Churchill, 1996). Composite interval mapping to assign significance based on the underlying trait distribution is robust at handling normal or near normal trait distributions (Rebai, 1997), as found for most of our phenotypes. The define.peak function implemented in the R/eqtl package was used to identify the peak location and one-LOD interval of each significant QTL for each trait (Wang et al., 2006). The effectscan function in the R/qtl package was used to estimate the QTL additive effect (R Development Core Team, 2014). Allelic effects for each significant QTL are presented as percent effect, by estimating $[\bar{x}_{Bay} - \bar{x}_{Sha}]/\bar{x}_{RIL}$ for each significant main effect marker.

QTL clusters or hot spots were identified using a QTL summation approach, where the position of each QTL for each trait was plotted on the chromosome by placing a 1 at the peak of the QTL. This was then used to sum the number of traits that had a detected QTL at a given position using a 5-cM sliding window across the genome (Kliebenstein et al., 2006). The significance threshold was determined using 1000 random permutations to determine QTL hot spots that were significant. Each QTL cluster was named with a representative marker close to the peak of the hot spot.

Additive ANOVA Model

To directly test the additive effect of each identified QTL cluster, an ANOVA model containing the markers most closely associated with each of the significant QTL clusters was used as individual main effect terms. For each growth phenotype, the mean phenotype in lines of genotype g at marker m under treatment t was shown as y_{gmt}. The model (additive model) for each phenotype in each line (y_{gmt}) was: $y_{gmt} = \mu + \sum_{m=1}^{m} 1 \sum_{t=1}^{2} TM_{tm} + \varepsilon_{gmt}$, where t = treatment: control or root constraint; m = markers 1, …,7. All growth phenotypes were tested with this model using lm function implemented in the R/car package, which returned all P values, Type III sums-of-squares for the complete model, and each main effect. QTL main-effect estimates (in terms of allelic substitution values) were estimated for each marker (Fox and Weisberg, 2011; R Development Core Team, 2014).

QTL Epistasis Analysis

To test directly for epistatic interactions between the detected QTLs, an ANOVA was conducted using the pairwise epistasis model. This pairwise epistasis model was used per growth phenotype because we had previous evidence that RIL populations have a significant false negative QTL detection issue and wanted to be inclusive of all possible significant loci (Chan et al., 2011). Within this model, all possible pairwise interactions between the markers and marker and treatment interactions were tested. For each phenotype, the average value in the RILs of genotype g at marker m in treatment t was shown as y_{gmt}. The model (pairwise epistasis model) for each metabolite in each line (y_{gmt}) was: $y_{g\,m\,t} = \mu + \sum_{t=1}^{2} 1 \sum_{m=1}^{m} M_{g\,m} + \sum_{t=1}^{2} 1 \sum_{m=1}^{m} \sum_{n=m+1}^{m} 1 T_t M_{g\,m} M_{g\,n} + \varepsilon_{g\,m\,n\,t}$, where t = control or root constraint; m = 1, …,7, and n is the identity of the second marker for an interaction. The main effect of the markers was denoted as M having a model involving seven markers. P values, Type III

sums-of-squares for the complete model, and each individual term and QTL pairwise-effect estimates in terms of allelic substitution values were obtained as described for additive model ANOVA (Fox and Weisberg, 2011; R Development Core Team, 2014). Significance values were corrected for multiple testing within a model using false discovery rate (<0.05). The main effect and epistatic interactions of the loci were visualized using cytoscape Version 2.8.3 with interactions significant for <10% of the phenotypes were excluded from the network analysis (Rowe et al., 2008; Smoot et al., 2011). The 10% threshold was chosen as an additional multiple testing correction to provide a more conservative image of the network. The same style of model was run to test for specific three-way interactions by including specific three-way terms as indicated (three-way epistasis model).

QTL Validation

The QTL effects were validated using HIFs (http://dbsgap.versailles.inra.fr/vnat/; Calenge et al., 2006) that overlapped with the QTL regions. HIF 364, overlapping with the QTL cluster (At2g14170; Figure 6A) and HIF 163 overlapping with the QTL cluster (At2g24150; Figure 6A) were used for validation. The HIF progeny with a Bay or Sha allele at the QTL region were grown under control and 0.5-cm root constraint. Since the *ELF3* genomic region overlapped with one of the QTL clusters (At2g24150; Figure 6A), previously available *ELF3* complementation lines (Jiménez-Gómez et al., 2010) were used to study the shoot responses to root constraint as described above. Two independent homozygous *ELF3* Bay or *ELF3* Sha transgenic lines were used. The growth conditions of the HIFs and *ELF3* complementation lines were kept similar to the QTL experiments. Plants were imaged and rosette diameter was measured as described above.

Accession Numbers

Sequence data from this article can be found in the Arabidopsis Genome Initiative and GenBank data libraries under accession number At2g25930 (*ELF3*).

Supplemental Data

Supplemental Figure 1. Response to complete root constraint.

Supplemental Figure 2. Response to various lengths of root constraints.

Supplemental Figure 3. Phenotypic variation in growth phenotype.

Supplemental Figure 4. Heritability of growth phenotypes.

Supplemental Data Set 1. The measured heritability of all measured growth phenotypes.

Supplemental Data Set 2. Model-based least square means for each RIL under control and root constriction used for QTL mapping.

Supplemental Data Set 3. Presentation of the ANOVA results for the main-effect model using the QTL markers.

Supplemental Data Set 4. Presentation of the P value results from the ANOVA using the QTL markers in a model involving QTL × QTL epistasis and QTL × treatment interactions.

Supplemental Data Set 5. Presentation of the Type III sums-of-square results from the ANOVA using the QTL markers in a model involving QTL × QTL epistasis and QTL × treatment interactions.

ACKNOWLEDGMENTS

This work was funded by National Science Foundation DBI Grant 0820580 to D.J.K., by National Science Foundation MCB Grant 1330337 to D.J.K., by the USDA National Institute of Food and Agriculture, Hatch project CA-D-PLS-7033-H to D.J.K., and by Danish National Research Foundation Grant DNRF99 to D.J.K.

AUTHOR CONTRIBUTIONS

B.J. and D.J.K. designed the research and wrote the article. B.J. and L.L. performed the research and analyzed the data.

Received April 22, 2015; revised July 6, 2015; accepted July 21, 2015; published August 4, 2015.

REFERENCES

Anwer, M.U., Boikoglou, E., Herrero, E., Hallstein, M., Davis, A.M., Velikkakam James, G., Nagy, F., and Davis, S.J. (2014). Natural variation reveals that intracellular distribution of ELF3 protein is associated with function in the circadian clock. eLife **3:** 3.

Badri, D.V., De-la-Peña, C., Lei, Z., Manter, D.K., Chaparro, J.M., Guimarães, R.L., Sumner, L.W., and Vivanco, J.M. (2012). Root secreted metabolites and proteins are involved in the early events of plant-plant recognition prior to competition. PLoS One **7:** e46640.

Beavis, W.D. (1994). The power and deceit of QTL experiments: lessons from comparative QTL studies. In Proceedings of the Forty-Ninth Annual Corn & Sorghum Industry Research Conference (Washington, DC: American Seed Trade Association), pp. 250–266.

Beavis, W.D. (1998). QTL analyses: power, precision, and accuracy. In Molecular Dissection of Complex Traits, A.H. Paterson, ed (New York: CRC Press), pp. 145–162.

Bernardo, R. (2004). What proportion of declared QTL in plants are false? Theor. Appl. Genet. **109:** 419–424.

Biedrzycki, M.L., Jilany, T.A., Dudley, S.A., and Bais, H.P. (2010). Root exudates mediate kin recognition in plants. Commun. Integr. Biol. **3:** 28–35.

Botto, J.F., Alonso-Blanco, C., Garzarón, I., Sánchez, R.A., and Casal, J.J. (2003). The Cape Verde Islands allele of cryptochrome 2 enhances cotyledon unfolding in the absence of blue light in Arabidopsis. Plant Physiol. **133:** 1547–1556.

Bouteillé, M., Rolland, G., Balsera, C., Loudet, O., and Muller, B. (2012). Disentangling the intertwined genetic bases of root and shoot growth in Arabidopsis. PLoS One **7:** e32319.

Cahill, J.F., Kembel, S.W., and Gustafson, D.J. (2005). Differential genetic influences on competitive effect and response in *Arabidopsis thaliana*. J. Ecol. **93:** 958–967.

Cahill, J.F., Jr., McNickle, G.G., Haag, J.J., Lamb, E.G., Nyanumba, S.M., and St Clair, C.C. (2010). Plants integrate information about nutrients and neighbors. Science **328:** 1657.

Calenge, F., Saliba-Colombani, V., Mahieu, S., Loudet, O., Daniel-Vedele, F., and Krapp, A. (2006). Natural variation for carbohydrate content in Arabidopsis. Interaction with complex traits dissected by quantitative genetics. Plant Physiol. **141:** 1630–1643.

Callaway, R.M., Pennings, S.C., and Richards, C.L. (2003). Phenotypic plasticity and interactions among plants. Ecology **84:** 1115–1128.

Chan, E.K., Rowe, H.C., Corwin, J.A., Joseph, B., and Kliebenstein, D.J. (2011). Combining genome-wide association mapping and transcriptional networks to identify novel genes controlling glucosinolates in *Arabidopsis thaliana.* PLoS Biol. **9:** e1001125.

Churchill, G.A., and Doerge, R.W. (1994). Empirical threshold values for quantitative trait mapping. Genetics **138:** 963–971.

Covington, M.F., Panda, S., Liu, X.L., Strayer, C.A., Wagner, D.R., and Kay, S.A. (2001). ELF3 modulates resetting of the circadian clock in Arabidopsis. Plant Cell **13:** 1305–1315.

de Kroon, H. (2007). Ecology. How do roots interact? Science **318:** 1562–1563.

de Wit, M., Kegge, W., Evers, J.B., Vergeer-van Eijk, M.H., Gankema, P., Voesenek, L.A.C.J., and Pierik, R. (2012). Plant neighbor detection through touching leaf tips precedes phytochrome signals. Proc. Natl. Acad. Sci. USA **109:** 14705–14710.

Doerge, R.W., and Churchill, G.A. (1996). Permutation tests for multiple loci affecting a quantitative character. Genetics **142:** 285–294.

Edwards, C.E., Ewers, B.E., McClung, C.R., Lou, P., and Weinig, C. (2012). Quantitative variation in water-use efficiency across water regimes and its relationship with circadian, vegetative, reproductive, and leaf gas-exchange traits. Mol. Plant **5:** 653–668.

Elwell, A.L., Gronwall, D.S., Miller, N.D., Spalding, E.P., and Brooks, T.L.D. (2011). Separating parental environment from seed size effects on next generation growth and development in Arabidopsis. Plant Cell Environ. **34:** 291–301.

Falik, O., Reides, P., Gersani, M., and Novoplansky, A. (2003). Self/non-self discrimination in roots. J. Ecol. **91:** 525–531.

Fang, S., Clark, R.T., Zheng, Y., Iyer-Pascuzzi, A.S., Weitz, J.S., Kochian, L.V., Edelsbrunner, H., Liao, H., and Benfey, P.N. (2013). Genotypic recognition and spatial responses by rice roots. Proc. Natl. Acad. Sci. USA **110:** 2670–2675.

Fox, J. and Weisberg, S. (2011). An R Companion to Applied Regression. (Thousand Oaks, CA: SAGE).

Freixes, S., Thibaud, M.C., Tardieu, F., and Muller, B. (2002). Root elongation and branching is related to local hexose concentration in *Arabidopsis thaliana* seedlings. Plant Cell Environ. **25:** 1357–1366.

Gersani, M., Abramsky, Z., and Falik, O. (1998). Density-dependent habitat selection in plants. Evol. Ecol. **12:** 223–234.

Hicks, K.A., Albertson, T.M., and Wagner, D.R. (2001). EARLY FLOWERING3 encodes a novel protein that regulates circadian clock function and flowering in Arabidopsis. Plant Cell **13:** 1281–1292.

Hodge, A. (2004). The plastic plant: root responses to heterogeneous supplies of nutrients. New Phytol. **162:** 9–24.

Jimenez-Gomez, J.M., Corwin, J.A., Joseph, B., Maloof, J.N., and Kliebenstein, D.J. (2011). Genomic analysis of QTLs and genes altering natural variation in stochastic noise. PLoS Genet. **7:** e1002295.

Jiménez-Gómez, J.M., Wallace, A.D., and Maloof, J.N. (2010). Network analysis identifies *ELF3* as a QTL for the shade avoidance response in Arabidopsis. PLoS Genet. **6:** e1001100.

Johanson, U., West, J., Lister, C., Michaels, S., Amasino, R., and Dean, C. (2000). Molecular analysis of FRIGIDA, a major determinant of natural variation in Arabidopsis flowering time. Science **290:** 344–347.

Joseph, B., Corwin, J.A., Züst, T., Li, B., Iravani, M., Schaepman-Strub, G., Turnbull, L.A., and Kliebenstein, D.J. (2013). Hierarchical nuclear and cytoplasmic genetic architectures for plant growth and defense within *Arabidopsis.* Plant Cell **25:** 1929–1945.

Karban, R., Baldwin, I.T., Baxter, K.J., Laue, G., and Felton, G.W. (2000). Communication between plants: induced resistance in wild tobacco plants following clipping of neighboring sagebrush. Oecologia **125:** 66–71.

Kellermeier, F., Chardon, F., and Amtmann, A. (2013). Natural variation of Arabidopsis root architecture reveals complementing adaptive strategies to potassium starvation. Plant Physiol. **161:** 1421–1432.

Kiaer, L.P., Weisbach, A.N., and Weiner, J. (2013). Root and shoot competition: a meta-analysis. J. Ecol. **101:** 1298–1312.

Kliebenstein, D.J., West, M.A., van Leeuwen, H., Loudet, O., Doerge, R.W., and St Clair, D.A. (2006). Identification of QTLs controlling gene expression networks defined a priori. BMC Bioinformatics **7:** 308.

Lankinen, A. (2008). Root competition influences pollen competitive ability in Viola tricolor: effects of presence of a competitor beyond resource availability? J. Ecol. **96:** 756–765.

Liu, B.-H. (1998). Statistical Genomics: Linkage, Mapping and QTL Analysis. (Boca Raton, FL: CRC Press).

Liu, X.L., Covington, M.F., Fankhauser, C., Chory, J., and Wagner, D.R. (2001). ELF3 encodes a circadian clock-regulated nuclear protein that functions in an Arabidopsis PHYB signal transduction pathway. Plant Cell **13:** 1293–1304.

Loudet, O., Chaillou, S., Camilleri, C., Bouchez, D., and Daniel-Vedele, F. (2002). Bay-0 x Shahdara recombinant inbred line population: a powerful tool for the genetic dissection of complex traits in Arabidopsis. Theor. Appl. Genet. **104:** 1173–1184.

Loudet, O., Chaillou, S., Krapp, A., and Daniel-Vedele, F. (2003a). Quantitative trait loci analysis of water and anion contents in interaction with nitrogen availability in *Arabidopsis thaliana.* Genetics **163:** 711–722.

Loudet, O., Chaillou, S., Merigout, P., Talbotec, J., and Daniel-Vedele, F. (2003b). Quantitative trait loci analysis of nitrogen use efficiency in Arabidopsis. Plant Physiol. **131:** 345–358.

Loudet, O., Gaudon, V., Trubuil, A., and Daniel-Vedele, F. (2005). Quantitative trait loci controlling root growth and architecture in *Arabidopsis thaliana* confirmed by heterogeneous inbred family. Theor. Appl. Genet. **110:** 742–753.

Michaels, S.D., and Amasino, R.M. (1999). FLOWERING LOCUS C encodes a novel MADS domain protein that acts as a repressor of flowering. Plant Cell **11:** 949–956.

Murphy, G.P., and Dudley, S.A. (2007). Above- and below-ground competition cues elicit independent responses. J. Ecol. **95:** 261–272.

Nieto, C., López-Salmerón, V., Davière, J.-M., and Prat, S. (2015). ELF3-PIF4 interaction regulates plant growth independently of the Evening Complex. Curr. Biol. **25:** 187–193.

Nord, E.A., Zhang, C., and Lynch, J.P. (2011). Root responses to neighbouring plants in common bean are mediated by nutrient concentration rather than self/non-self recognition. Funct. Plant Biol. **38:** 941–952.

Padilla, F.M., Mommer, L., de Caluwe, H., Smit-Tiekstra, A.E., Wagemaker, C.A.M., Ouborg, N.J., and de Kroon, H. (2013). Early root overproduction not triggered by nutrients decisive for competitive success belowground. PLoS One **8:** e55805.

Paul-Victor, C., Züst, T., Rees, M., Kliebenstein, D.J., and Turnbull, L.A. (2010). A new method for measuring relative growth rate can uncover the costs of defensive compounds in *Arabidopsis thaliana*. New Phytol. **187:** 1102–1111.

R Development Core Team (2014). R: A Language and Environment for Statistical Computing. (Vienna, Austria: R Foundation for Statistical Computing).

Rebai, A. (1997). Comparison of methods for regression interval mapping in QTL analysis with non-nomral traits. Genet. Res. **69:** 69–74.

Rowe, H.C., Hansen, B.G., Halkier, B.A., and Kliebenstein, D.J. (2008). Biochemical networks and epistasis shape the *Arabidopsis thaliana* metabolome. Plant Cell **20:** 1199–1216.

Roycewicz, P., and Malamy, J.E. (2012). Dissecting the effects of nitrate, sucrose and osmotic potential on Arabidopsis root and shoot system growth in laboratory assays. Philos. Trans. R. Soc. Lond. B Biol. Sci. **367:** 1489–1500.

Semchenko, M., Zobel, K., Heinemeyer, A., and Hutchings, M.J. (2008). Foraging for space and avoidance of physical obstructions

by plant roots: a comparative study of grasses from contrasting habitats. New Phytol. **179:** 1162–1170.

Slovak, R., Göschl, C., Su, X., Shimotani, K., Shiina, T., and Busch, W. (2014). A scalable open-source pipeline for large-scale root phenotyping of Arabidopsis. Plant Cell **26:** 2390–2403.

Smith, H. (2000). Phytochromes and light signal perception by plants–an emerging synthesis. Nature **407:** 585–591.

Smoot, M.E., Ono, K., Ruscheinski, J., Wang, P.-L., and Ideker, T. (2011). Cytoscape 2.8: new features for data integration and network visualization. Bioinformatics **27:** 431–432.

Torii, K.U., Mitsukawa, N., Oosumi, T., Matsuura, Y., Yokoyama, R., Whittier, R.F., and Komeda, Y. (1996). The Arabidopsis ERECTA gene encodes a putative receptor protein kinase with extracellular leucine-rich repeats. Plant Cell **8:** 735–746.

Tosti, G., and Thorup-Kristensen, K. (2010). Using coloured roots to study root interaction and competition in intercropped legumes and non-legumes. J. Plant Ecol. **3:** 191–199.

Undurraga, S.F., Press, M.O., Legendre, M., Bujdoso, N., Bale, J., Wang, H., Davis, S.J., Verstrepen, K.J., and Queitsch, C. (2012). Background-dependent effects of polyglutamine variation in the *Arabidopsis thaliana* gene ELF3. Proc. Natl. Acad. Sci. USA **109:** 19363–19367.

Valladares, F., Gianoli, E., and Gómez, J.M. (2007). Ecological limits to plant phenotypic plasticity. New Phytol. **176:** 749–763.

Wang, S., Basten, C.J., and Zeng, Z.-B. (2006). Windows QTL Cartographer 2.5. (Raleigh, NC: North Carolina State University).

Wentzell, A.M., Boeye, I., Zhang, Z., and Kliebenstein, D.J. (2008). Genetic networks controlling structural outcome of glucosinolate activation across development. PLoS Genet. **4:** e1000234.

Wentzell, A.M., and Kliebenstein, D.J. (2008). Genotype, age, tissue, and environment regulate the structural outcome of glucosinolate activation. Plant Physiol. **147:** 415–428.

West, M.A., van Leeuwen, H., Kozik, A., Kliebenstein, D.J., Doerge, R.W., St Clair, D.A., and Michelmore, R.W. (2006). High-density haplotyping with microarray-based expression and single feature polymorphism markers in Arabidopsis. Genome Res. **16:** 787–795.

West, M.A.L., Kim, K., Kliebenstein, D.J., van Leeuwen, H., Michelmore, R.W., Doerge, R.W., and St Clair, D.A. (2007). Global eQTL mapping reveals the complex genetic architecture of transcript-level variation in Arabidopsis. Genetics **175:** 1441–1450.

Züst, T., Joseph, B., Shimizu, K.K., Kliebenstein, D.J., and Turnbull, L.A. (2011). Using knockout mutants to reveal the growth costs of defensive traits. Proc. Biol. Sci. **278:** 2598–2603.